Environmental Science and Pollution Research (2023) 30:32710–32721
https://doi.org/10.1007/s11356-022-24238-4

RESEARCH ARTICLE

Improving the performance of a modified solar distiller with phase change material and parabolic trough collector

Mishal Alsehli[1]

Received: 24 September 2022 / Accepted: 12 November 2022 / Published online: 5 December 2022

Abstract

The solar stills can solve the problem of freshwater shortage for the people living in remote areas. Through this work, the performance of hybrid solar desalination arrangement was investigated. The system comprised of parabolic trough solar collector, automatic solar tracking system, separation room, modified solar still, two condensation units, feed water tank, and supplementary and measuring tools. The effect of using various water flow rates on the effectiveness of parabolic trough solar collector was tested. Also, the influences of integrating condenser to the modified solar still with and without phase change material were studied. The experimental results revealed that the best flow rate for parabolic trough solar collector was obtained as 10 L/h (100 L/day), where its effectivity was 61%. Under this condition, the obtained freshwater was around 61 L/day from a total saline water of 100 L/day. In addition, integrating a condenser to the modified solar still improved its productivity. So, the total yields of conventional and modified solar stills were 2500 and 5145 mL/m^2.day, respectively. Therefore, the distillate of modified solar still was improved by 105.8% as compared to that of the conventional solar still due to using the hot feed water and external condenser. Moreover, using phase change material enhanced the modified solar still yield. The total yield of conventional solar still and modified solar still with hot feed water, condenser, and phase change material was 2575 and 6150 mL/m^2.day, respectively. Consequently, the productivity of the modified solar still with hot feed water, condenser, and phase change material was improved by around 138.83% over that of the conventional solar still. Finally, the conventional solar still had an average efficiency of 31.5%. Also, when using the hot feed water and external condenser with the modified solar still, the thermal efficiency was reported as 49.7%. Also, the modified solar still with hot water, condenser, and phase change material had a thermal efficiency of 56.5%. Finally, the water costs of 1 L from the CSS and MSS are 0.063 $ and 0.050 $, respectively.

Keywords Collector · Condensation · Separation · Distillation · Phase change material

Abbreviations

ASTS	Automatic solar tracking system
CSS	Conventional solar still
CU	Condensation unit
EP	Evacuated pipe
FWT	Feed water tank
HDH	Humidification-dehumidification
MSS	Modified solar still
MSTM	Manual solar tracking mechanism
PCM	Thermal storage material
PTSC	Parabolic trough solar collector
PWPCM	Paraffin wax phase change material
SR	Separation room

Responsible Editor: Philippe Garrigues

✉ Mishal Alsehli
m.alsehli@tu.edu.sa

[1] Department of Mechanical Engineering, College of Engineering, Taif University, P.O. Box 11099, Taif 21944, Saudi Arabia

Introduction

As well known, the sea water desalination systems are widely employed all over the world due to the problem of freshwater shortage. In addition, the solar energy, as a renewable energy, was introduced as a cost reducing tool for the desalination systems. Therefore, the various desalination systems such as humidification-dehumidification (HDH), stage flashing, freezing, and solar distillation are found in the literature (Essa 2022; Tiwari and Sahota 2017). Also,

the scholars tried to improve the solar distillation systems by introducing numerous amendments (Shanmugan et al. 2020).

One of the main solar concentrating devices is the parabolic trough solar collector (PTSC) which concentrates the solar radiation on a predesigned line. For this purpose, PTSC was utilized as a preheater for the solar stills. The various PTSC applications with dish concentrators were reviewed for solar-powered desalination units by Aboelmaaref et al. (Aboelmaaref et al. 2020). In another work (Makkeh et al. 2020), PTSC was applied as a heat source for Rankine cycle which produced energy to run a reverse osmosis plant. This reduced the permeate cost by 23%, and the CO_2 emission was eliminated by 52,164 tons/year. Besides, Mosleh et al. (Mosleh et al. 2015) used heat pipes with PTSC to get distilled water, and they obtained 0.933 L/(m^2.h) and achieved system efficacy of 65.2%. Also, the life cycle cost of solar desalination plant (stage flashing unit) powered by PTSC was tested by Ziyaei et al. (Ziyaei et al. 2021). The authors reported that the proposed units powered by solar energy and natural gas and installed in Hurghada, Egypt, had the fewest cycle cost due to providing 88% of requested power from the sun. Moreover, decreasing the saline water pH was conducted via using PTSC (Narayanan and Vijay 2020), where it was reduced to 7.301–7.5878 regarding the water temperature.

On the other hand, the solar still is a simple device used for providing potable water from saline or brackish water. But, it was reported that the solar distiller uses only 38.40% of the total incident solar power for evaporation purpose which is the main principal of solar distillers (Ranjan et al. 2016). While the remaining solar power is considered as thermal losses. Regarding this fact, the scholars proposed using the thermal storage materials (PCM) to eliminate the thermal losses from the distiller (Amarloo and Shafii 2019). Moreover, the paraffin is a well-known material used in thermal systems due to its thermal storing properties. Faghiri et al. (Faghiri et al. 2021; Hosseininaveh et al. 2021) improved the solidification process of the paraffin PCM with the help of using acetone droplet onto molten paraffin surface. They found that as the drop hits the paraffin surface, acetone begins to boil, and a portion of paraffin begins to solidify. In another study (Faghiri et al. 2022), the authors tested the optimization of parameters for acetone droplet impingement on paraffin PCM. In addition, the PCM stores thermal energy through the high solar intensity times and releases it during the times of clouds or absence of sun. For instance, Srithar (Srithar 2010) raised the distiller productivity by 32.32% via utilizing the PCM of sand and sponge. Moreover, Abdelgaied et al. (Abdelgaied et al. 2021) used a PCM with fins to enhance the productivity of tubular distiller. The distillate was augmented by 90.1%, where it reached 7.89 L/m^2.day. Besides, Essa et al. (Essa et al. 2022) improved the distillate of a tubular distiller using PCM, concentrator, and rotational drum. The results revealed that the distiller productivity was augmented by 218%, and thermal efficacy reached 63.8%. In another publication (Abdullah et al. 2022), the productivity of tubular distiller was enhanced via using nano-coating and nano-PCM. The authors increased the distiller yield by 34% when using Ag nanoparticles with the PCM. Furthermore, Madhlopa and Johnstone (Madhlopa and Johnstone 2009) numerically modelled the performance of a passive distiller with external condenser. Using the condenser with the distiller raised its productivity by 62%. Also, Hassan and Abo-Elfadl (Hassan and Abo-Elfadl 2017) used various kinds of condensers integrated with a single solar distiller. They reported an increase in distiller productivity by 52% when using heat sink condenser with black steel fibers in the basin. Emran et al. (Emran et al. 2022) integrated the triangle solar distiller with a heater and condenser to improve its performance under Malaysian environmental conditions. These modifications augmented the productivity of distiller by 24%. Besides, Grewal and Kumar (Grewal &Kumar) tested the thermo-enviro-economic performances of stepped distiller with various masses of PCM (0.45, 0.90, and 1.35 L). The authors concluded that the more the mass of PCM was, the more the productivity was. The distiller productivity was obtained as 2.18 L with an increase of 8.4%, and the efficiency reached 31.53%.

The present work aims at enhancing the performance of a hybrid solar desalination system. This system consists of a parabolic trough solar collector (PTSC) with automatic solar tracking system (ASTS), separation room (SR), modified solar still (MSS) with manual solar tracking mechanism (MSTM), two condensation units (CU), feed water tank (FWT), and supplementary and measuring tools. This arrangement optimizes the use of both systems due to using the exhaust of PTSC as a feed for the MSS. Also, the PTSC was used as an energy source for the MSS. The saline water is heated by the PTSC to a high temperature which was enough to get vapor. This vapor was condensed through one of the CUs which was connected to the SR. Also, the exhaust of PTSC was free to feed the MSS with brine water at high temperature. The MSTM was achieved by considering all walls of MSS from glass. This allows the distiller to absorb more solar radiation. Also, the MSS was structured with an external CU to amend its condensation and evaporation rates. Finally, a phase change material of paraffin wax (PWPCM) was used under the basin liner of the MSS to enhance its evaporation. The novelty points of this work, which differ from the other relevant publications, can be listed below.

1. As expected, the performance of the hybrid desalination system depends on the water flow rate of PTSC. So, the effect of using various water flow rates of (5, 10, 15, 20, 25, and 35 L/h) through the PTSC on the system performance was tested.
2. The influence of using external condensation unit on the performance of the hybrid desalination system was studied.

3. The impact of utilizing paraffin wax phase change material (PWPCM) on the performance of the hybrid desalination system was examined. The PWPCM was placed under the basin liner of the MSS.

Experimental considerations

Design and fabrication

The investigated desalination unit consists of a parabolic trough solar collector (PTSC) with automatic solar tracking system (ASTS), modified solar still (MSS) with manual solar tracking mechanism (MSTM), two condensation units (CU), feed water tank (FWT), and supplementary and measuring tools. Figure 1 illustrates the components of experimental work. The diameter and length of FWT were 50 cm and 50 cm, respectively.

As obtained from Fig. 1, the PTSC has a parabolic shape. The fabrication details of PTSC parameters are presented in Table 1. The external PTSC frame was made of wood due to its lightness and cheapness. The wooden frame was lined with a reflector, which was made of stainless steel 201 (0.4 mm thick). Then, a metal support was used to fix the PTSC frame. To achieve the purpose of solar tracking, the metal support was able to rotate the PTSC by 360° to make sure of tracking the sun. The selection of basic design factors for PTSC was regarded to keep desirable efficacy, facility design, and keep low cost. Moreover, an evacuated pipe (EP) was fixed at the center line (focal point) of the PTSC. The EP was fabricated of two concentric tubes with vacuum between them. The purpose of vacuum layer is to extinguish the heat loss and keep good efficiency of PTSC. The EP had 47 and 58 mm inner and outer diameters, respectively with a length of 1.8 m. The water flows through the inside pipe (U-shape copper pipe) of EP.

Furthermore, an automatic solar tracking system was utilized with the PTSC to make sure following the direct solar beams as possible (Fig. 1). The tracking mechanism had a single-tracking axis (North–South axis) to direct the PTSC through the direct incident solar rays. The main components of the tracking scheme were a DC motor, speed simplification pattern, exposure resistor sensing sample, and controller. The exposure sensing sample had two resistors for solar radiation fixed at the East and West sides of PTSC mirror. This sensing unit produces a voltage difference relative to the solar radiation incident angle. Then, the controller translates this voltage difference into rotational movement until the voltage difference goes back to zero to stop PTSC rotation, and so on.

Table 1 Design details of PTSC factors

Factor	Value and unit
Receiver minimal diameter	4.65 mm
Rim radius	500 mm
Rim angle	90°
Concentration ratio	6.77
Focal height	250 mm
Width of parabola	1 m

Additionally, a separation room (SR) was connected to the exit of EP as shown in Fig. 1. The fluid inside the SR is a mixture of hot water and steam. The hot water was allowed to feed the MSS, while the steam was drawn back to be distilled into an outside condenser connected to SR. The SR uses the gravitational force to separate the denser fluid (liquid) from the less dense fluid (vapor), where the liquid settles at the bottom of SR, while the steam rises to the top of the room as its density is lighter than the liquid and is drawn to be condensed in the condensation unit. The SR was well insulated to prevent the heat loss to ambient.

Besides, the test-rig was boosted by a modified solar still (MSS) to use the reject hot water from the SR as illustrated in Fig. 1. The design and fabrication details of the MSS are presented in Table 2. The solar still was amended by considering some points. First, the MSS vertical walls were made of glass

Fig. 1 Photo of investigated experimental setup

Table 2 Design and fabrication details of the modified solar still

Parameter	Value & unit
Width	50 cm
Length	100 cm
Smallest wall height	15 cm
Glass cover tilt angle	30°
Material of fabrication	Galvanized steel and glass sheets
Thickness of fabrication material	1.5 mm
Number of fixed troughs	3 troughs
Sides of glass	East, South, and West sides
Sides of galvanized steel	North and bottom sides
Cover of distiller	Single glass cover
Number of used thermocouples	9 thermocouples (2 for glass, 2 for basin liner, 2 for basin water, 1 for vapor, and 2 for glass walls)

Table 3 Details and uncertainty of measuring tools

Instrument	Target (unit)	Resolution	Accuracy	Range	Error
Waterproof temperature sensing elements	Temperature (°C)	0.1	±0.5 °C – ±2 °C	-50 – 100 (°C)	1.3%
DHT11 temperature meter	Temperature (°C)	0.1	±1 °C	0 – 50 (°C)	1.1%
K-type thermocouples	Temperature (°C)	0.1	±0.5 (°C)	0 – 200 (°C)	1.3%
Solarimeter	Solar intensity (W/m^2)	0.1	±5 (W/m^2)	0 – 5000 (W/m^2)	1.6%
Wind speed measuring tool GM8908	Ambient air velocity (m/s)	0.01	±0.10 (m/s)	0.4 – 30 (m/s)	1.4%
Calibrated flasks	Distillate (L)	0.5	±5 (mL)	0 – 2500 (mL)	1.5%

to track the solar rays manually. Only the back wall (North side) of MSS was made of galvanized steel due to the lower incident solar radiation from this side. Second, the MSS was integrated with an external condensation unit with suction fan.

As explained above, two CUs were connected to the desalination system. One CU was installed after the SR, and the other CU was integrated to the MSS. Each CU comprises two enclosed aluminum vessels to store the cooling medium (cold water). Also, a copper serpentine was used to carry the vapor to be condensed. This serpentine passes inside the inner vessel of CU. In addition, four fixed holes were found in each CU: two for cooling medium, one for vapor, and one for condensed water.

Testing instruments and uncertainty analysis

The performance of the desalination system can be evaluated by measuring its affecting parameters such as the temperature, solar radiation, ambient air velocity, and distillate quantity. As a result, the waterproof temperature sensing elements were utilized to know the values of water, steam, and condenser temperatures. Also, the ambient air temperature was measured by DHT11 temperature meter. In addition, the temperature of compartments inside the MSS was recorded using K-type thermocouples. All temperature meters were integrated to ARDUINO mega 2560 (54 digital points) to read the digital value of temperatures. Moreover, the solar intensity was reported using a Solarimeter. Besides, the ambient air velocity was measured by a wind speed measuring tool GM8908. Finally, the calibrated flasks were utilized to record the distillate quantities. All required information about the measuring tools is presented in Table 3.

Due to making an experimental work, the error analysis was mandatory to be conducted for the measuring tools. The technique used by Holman (Holman 2012) is followed to calculate the errors derived in the calculations of efficiency. This technique estimates the error as obtained in the following relations:

$$W_R \text{ (result uncertainty)} = \sqrt{\left(\frac{\partial R}{\partial X_1}W_1\right)^2 + \left(\frac{\partial R}{\partial X_2}W_2\right)^2 + \cdots + \left(\frac{\partial R}{\partial X_n}W_n\right)^2} \quad (1)$$

where W_1, W_2, W_3, ……, W_n refer to the independent variables' uncertainties. The resulting errors are demonstrated in Table 3. Furthermore, as the yield is a function of the depth of water (m = f(h)), its uncertainty is

$$W_m(\text{uncertainty in the distillate}) = \sqrt{\left(\frac{\partial m}{\partial h_1} W_h\right)^2} \quad (2)$$

where, m is the distillate yield, and h is the depth of water.

Besides, as the distiller efficiency (η_{th}) depends on the solar radiation (I(t)) and distillate, its uncertainty is

$$W_{\eta_{th}}(\text{uncertainty in efficiency}) = \sqrt{\left(\frac{\partial \eta_{th}}{\partial m} W_m\right)^2 + \left(\frac{\partial \eta_{th}}{\partial I_R} W_{I(t)}\right)^2} \quad (3)$$

So, the errors derived for the productivity and efficiency are around ± 1.7% and ± 2.8%, respectively.

Procedures and steps of tests

The desalination system was assembled and tested in Taif, Saudi Arabia. Then, the tests came into the following steps.

1. The first stage of experiments was testing the effect of various water flow rates (5, 10, 15, 20, 25, and 35 L/h) through the PTSC on the system performance. The saline feed water enters the evacuated tube of PTSC and gets hot by the incident solar radiation. After that, a separation process for the water and steam was conducted in the separation room. The exit water from the SR was employed as feed for MSS. In this stage, the best flow rate (BFR) for PTSC was determined.
2. In the second stage of experiments, the system was operated at the BFR. Also, the MSS was integrated with an outside condenser to amend its performance. CU withdraws the excess vapor from the MSS to be condensed outside the distiller. This is expected to improve the system performance.
3. The last step of experimentations was using the phase change material of paraffin wax (PWPCM) under MSS basin. Using PWPCM improves the evaporation rate of the MSS, and hence the total distillate of the desalination system will be augmented. The properties of the PWPCM are tabulated in Table 4. Also, the Differential Scanning Calorimetry (DSC) curves of PWPCM are obtained in Fig. 2.

Results and discussion

Impact of different water flow rates on EP effectivity

Here, the impact of flowing saline water inside the EP at various flow rates on the system performance was examined.

Table 4 Thermo-physical properties of paraffin wax

Dimension	Paraffin wax
Density, kg/m^3	876
Melting point, ºC	53
Latent heat of fusion, kJ/kg °C	190
Specific heat, kJ/kg °C	2.1
Thermal conductivity, W/m °C	0.21

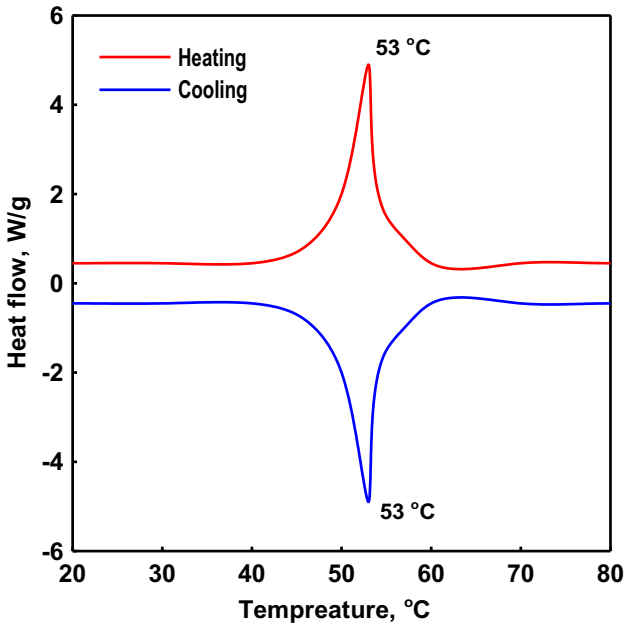

Fig. 2 DSC curves of the paraffin wax PCM (PWPCM)

The yields (distillate productivity and total daily input flow) and temperature of the system at different flow rates are illustrated in Table 5. It is worth to mention that these tests were conducted at different days but under similar environmental conditions. Hence, the average value of solar intensity for all tests was around ~ 700 W/m^2 as shown in Table 5. This point was important to be achieved to make sure the reliability of results. It can be concluded from Table 5 that the temperature of saline water exiting from the EP strongly depended on the saline water flow rate. As a result, the temperature of flowing water is declined with increasing the flow rate of water through the EP. For instance, the maximum temperature of saline water was approximately 92 °C, 86 °C, and 81 °C at the saline water flow rates 5, 10, and 15 L/h, respectively. Therefore, the greater the saline water flow rate through the EP, the fewer the temperature of saline at the exit of the EP as observed from Table 5. The explanation of this phenomenon is based on the fluid mechanics rationales. Regarding the continuity equation for liquids,

Table 5 Conditional details of the EP effectivity and outlet temperature under different water flow rates

Case	Flow rate of water (L/h)	Daily flowing quantity (L/day)	Distilled water (L/day)	EP effectivity (%)	Outlet water temperature (°C)
1	5	50	26.5	53	92
2	10	100	61	61	86
3	15	150	84	56	81
4	20	200	86	43	70
5	25	250	82.5	33	62
6	35	350	73.5	21	49

$$Q(\text{volume flow rate}) = A(\text{cross sectional area}).\text{V}(\text{normal velocity}) \quad (4)$$

and for constant EP diameter ($D = 47\text{mm}$), then the cross-sectional area (A) would have a constant value. Therefore, increasing the volume flow rate of saline water would increase its velocity. Besides, increasing the saline water velocity means that the time that a certain amount of water would spend inside the tube that would be exposed to solar radiation (the source of warming the water) would be less than it would be if the water velocity was lower. As a result, increasing the saline water flow rate raised its flowing velocity, and hence the water temperature was declined as seen in Table 5 due to shortening the time that the water would stay be focused under the sun rays of PTSC. As a result, the water temperature was declined from 92 °C at 5 L/h, to 86 °C at 10 L/h, to 70 °C at 20 L/h, and to 49 °C at 35 L/h. On the second hand, it can be concluded from Table 5 that the amount of freshwater distillate obtained strongly depends on the saline water flow rate. In addition, the saline water temperature significantly affects the output freshwater yield of EP. This is because the fact that the evaporation process would be conducted in a better way if the water temperature is high rather than the case of low water temperature. So, raising the saline water temperature inside the EP would improve the evaporation process of the pipe. Then, the quantity of the output yield of EP would be greater if it is condensed well. To evaluate the individual performance of EP alone, the authors would like to identify the EP effectivity parameter, which can be explained as the percentage of the obtained output yield over the total input quantity of water to the EP.

According to Eq. (5), the EP effectivity under different water flow rates can be calculated as tabulated in Table 5. It can be obtained from Table 5 that the output distillate from the EP mainly depends on the saline water flow rate. When the saline water flow rate was 5 L/h (50 L/day), the distillate was around 26.5 L/day, and the EP effectivity was around 53%, while the distillate and EP effectivity were 61 L/day and 61% for the saline water flow rate of 10 L/h (100 L/day). After that, the amount of distillate increased with increasing the flow rate, but the EP effectivity begins to decrease as shown in Table 5. For instance, at the flow rate 15 L/h (150 L/day), the EP effectivity was 56% (Table 5). Also, EP effectivity was 43%, 33%, and 21% for the saline water flow rates 20, 25, and 35 L/h, respectively (Table 5). In addition, the productivity of EP was 84, 86, 82.5, and 73.5 L/day at the flow rates 15, 20, 25, and 35 L/h, respectively. Regarding the above results, the best flow rate (BFR) for PTSC was obtained as 10 L/h (100 L/day).

Performance of MSS with condenser and EP at BFR

In this section, the system was operated at the BFR of the EP. Also, the MSS was structured with condenser to amend its performance. CU withdraws the excess vapor from the MSS to be condensed outside the distiller. The MSS was enriched by the hot brine rejected from the separation unit installed after the EP.

The solar radiation, wind speed, and temperatures of water and glass of both solar stills (conventional solar still CSS and MSS with hot feed water and condenser) are presented in Fig. 3. The maximal values of irradiance and temperatures were observed at noon time (≈12:00). The

$$\text{EP effectivity}, \% = \frac{\text{Amount of distillate from EP (L/day)}}{\text{Total quantity of saline water input to EP (L/day)}} \times 100 \quad (5)$$

irradiance increased from 635 W/m^2 at 09:00 to 1050 W/m^2 at 12:00. In the afternoon, the irradiance declined to record 200 W/m^2 at 18:00 (Fig. 3). In addition, the temperature profiles were the same as the solar irradiance. The ambient temperature was raised from 29 °C at 09:00 to 39 °C at 12:00, and this was the maximum surrounding air temperature. After that, the ambient temperature began to be declined with decreasing the solar irradiance and

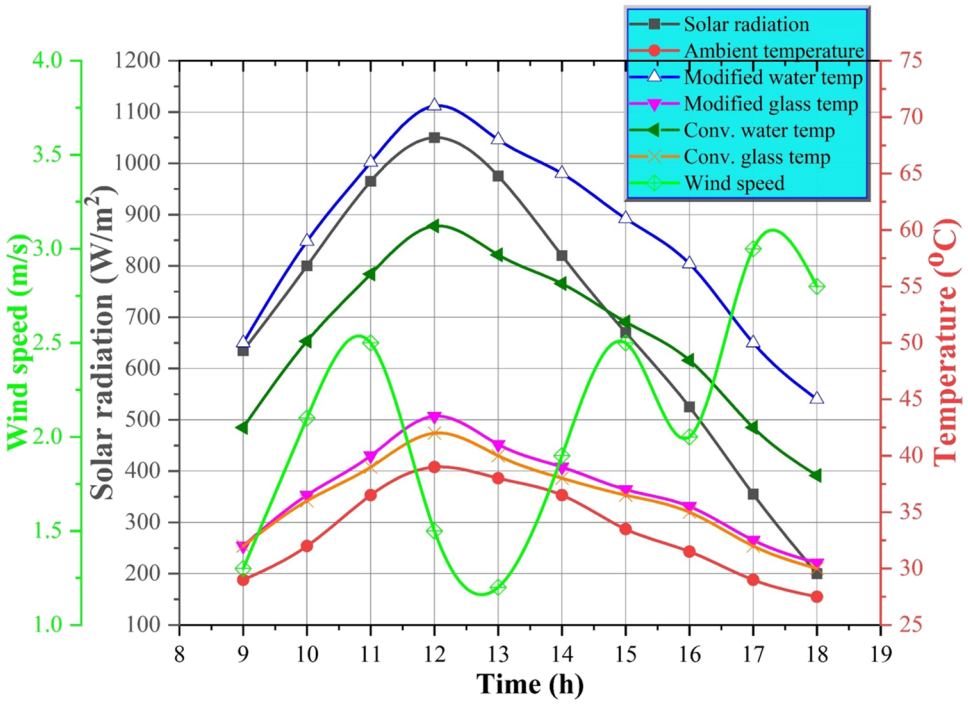

Fig. 3 Solar radiation, wind speed, and temperatures of water and glass of both solar stills

reported its minimum value of 27.5 °C at 18:00 (Fig. 3). It was observed from Fig. 3 that the change occurred in the ambient temperature was limited to 11.5 °C through the whole day from the morning to sunset. Also, this change in ambient temperature was referred to the change in solar radiation. For the effect of ambient wind speed on the solar distiller performance, it was observed from Fig. 3 that the affecting-performance parameters of solar stills did not depend on the ambient air speed. This is due to that the wind speed changed from 1.3 m/s to 3 m/s, and this change did not appear on the water and glass temperatures (Fig. 3).

On the second hand, the water and glass temperatures strongly rely on the solar irradiance and follow its behavior as presented in Fig. 3. Also, it was observed from Fig. 3 that the temperature of water of MSS with hot feed water and condensation was more than that of CSS. This is intuitively expected because the distiller is fed with hot water coming from the EP. As well known, the more the temperature of water, the more the evaporation content of the distiller. The water temperature increased from 50 °C at 09:00 to 71 °C at 12:00 and from 42.5 °C at 09:00 to 60 °C at 12:00 for both MSS and CSS, respectively (Fig. 3). Then, in the afternoon, the water temperature began to be declined with decreasing the solar irradiance as illustrated in Fig. 3. The lowest water temperature was observed at the end of testing (18:00), where it was 45 °C and 38 °C for MSS and CSS, respectively. Thus, the temperature of water of MSS was more than that of CSS by around 6.5–11 °C. This difference in water temperature makes the MSS generated more vapor over that of CSS.

As well known, the more the evaporation inside a distiller, the more the glass temperature of the same distiller. This means that increasing the vaporization of still raises the glass temperature; thus, the water–glass temperature difference becomes lower, and this badly affects the solar still productivity. As a result, the author preferred to integrate an external condenser with the MSS to withdraw some vapors from the MSS and condensate them outside the distiller. This design would lead to reduce the glass temperature due to diminishing the thermal loading on the glass inside surface. Figure 3 illustrates that the MSS glass temperature was more than that of CSS with a little value. As a result, the difference in glass temperature of MSS and CSS was around 0–1.5 °C (Fig. 3). Therefore, it can be said that the glass temperature of MSS without condenser would be higher than that of the MSS with condenser. So, using the condenser with MSS reduced its glass temperature, which improved the condensation. Then, the evaporation and condensation rates of MSS were improved well; thus, the MSS performance would be improved.

Furthermore, the hourly variations of productivity and accumulated yield of both distillers and EP are illustrated in Fig. 4. It can be observed from Fig. 4 that the hourly productivity of MSS with hot feed water and condenser was more than that of the CSS. Also, the hourly productivity started from zero at the beginning of experiments and increased gradually to reach its maximum value at noon (12:00). After that, the productivity began to be reduced dramatically till the end of tests. For instance, the hourly yield of MSS increased from zero at 09:00 to 780 mL/m^2.h at 12:00,

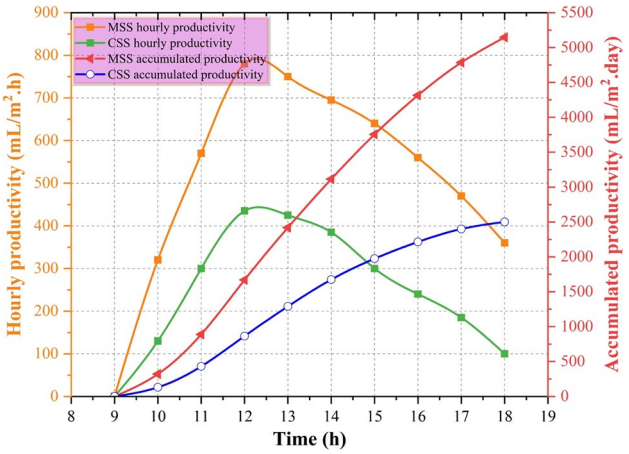

Fig. 4 The variations of hourly and accumulated productivities of both distillers

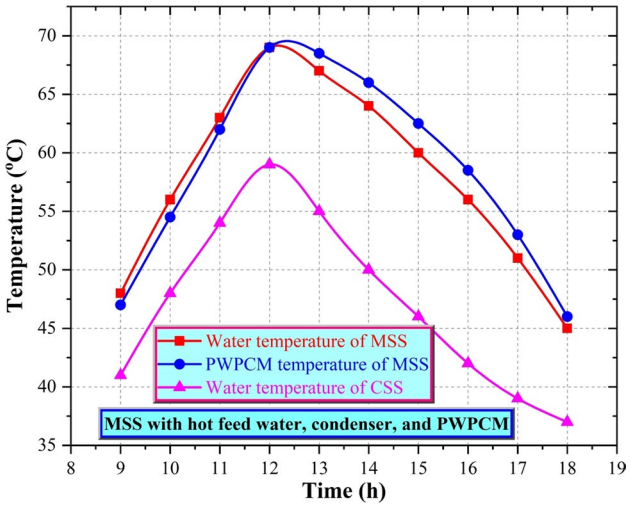

Fig. 5 The water and PCM temperatures for MSS compared to water temperature of CSS

while the hourly productivity of CSS increased from zero at 09:00 to 435 mL/m^2.h at 12:00 (Fig. 4). After that, the yields of MSS and CSS were decreased to report 360 and 100 mL/m^2.h at 18:00, respectively (Fig. 4). Also, it can be seen from Fig. 4 that productivity of MSS had a decrease slope smaller than that of the CSS in the period from afternoon to sunset. Therefore, the productivity of MSS was greater than that of the CSS as presented in Fig. 4. This was due to the following reasons. The MSS was fed by hot water, which increases its vaporization rate. Also, integrating the MSS with external condenser improves the condensation rate due to enlarging the temperature difference between the water and glass. Besides, the condenser fan removed part of the thermal load on the glass, which decreases its temperature as obtained from Fig. 3. Moreover, the fan created a turbulence in the vapor content inside the MSS. This could enhance the evaporation sue to improving the heat transfer characteristics. In addition, the impact of non-condensable gases is eliminated with the help of using the fan, which withdraws them outside the MSS. Therefore, the MSS fed by hot water and integrated with condenser had a distillate greater than that of the CSS as shown in Fig. 4.

Additionally, the accumulated yield of MSS with hot feed water and condenser was higher than that of the CSS as obtained from Fig. 4. The total productivities of CSS and MSS were 2500 and 5145 mL/m^2.day, respectively. As a consequence, the distillate of MSS was improved by 105.8% over that of the CSS due to using the hot feed water and external condenser.

Performance of MSS with phase change material

Here, the effect of using phase change material of paraffin wax (PWPCM) under the basin liner of the MSS was tested. Using PWPCM would improve the evaporation rate of the MSS, and hence the total distillate of the desalination system will be augmented. To correctly evaluate the impact of using PWPCM with the desalination system, the temperature of PWPCM was monitored hourly and compared to the water temperature of MSS. So, the hourly changes of water and PWPCM temperatures for MSS are obtained in Fig. 5. It is observed from Fig. 5 that the temperature follows the same behavior explained above. As the solar radiation increases, the temperature increases, and vice versa. The maximum temperature was noticed at noon time (12:00) as obtained from Fig. 5. Also, it is revealed that the PWPCM takes heat in from the neighboring hot water through the times of water temperature increase or solar radiation increase. This phenomenon of warming the PWPCM up is called as heating process of PWPCM. Through this process, the PWPCM temperature was lower than the basin water temperature by around 0–1.5 °C. For instance, the water and PWPCM temperatures were 48 °C and 47 °C respectively at 09:00, and they increased to reach 69 °C each at 12:00 as shown in Fig. 5. The reason behind equalizing the water and PWPCM temperatures at 12:00 maybe that the time of sourcing thermal energy to the water and PWPCM is ended at 12:00, and the water becomes a heat sink from PWPCM instead of being a heat source for PWPCM. After the maximum temperature reached by the PWPCM (around 12:00), the slope of the PWPCM temperature curve was inverted to begin giving heat to the water instead of taking it in. Therefore, a discharge process for the thermal energy stored by PWPCM begins to work. As a result, the PWPCM temperature starts to be decreased as shown in Fig. 5 for the period of afternoon. Besides, the PWPCM temperature was higher than that of the water temperature of MSS through the period of afternoon (discharge process). The water temperature was

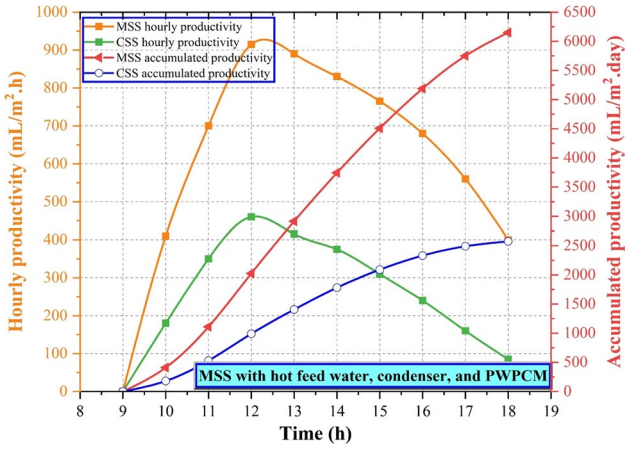

Fig. 6 The hourly and accumulative yields of CSS and MSS with hot feed water, condenser, and PWPCM

declined from 69 °C at 12:00 to 45 °C at 18:00, while the PWPCM temperature was declined from 69 °C at 12:00 to 46 °C at 18:00. Thus, the PWPCM temperature was higher than the basin water temperature by around 0–2.5 °C through the discharge process (from 12:00 to 18:00).

Moreover, the hourly and accumulative yields of CSS and MSS with hot feed water, condenser, and PWPCM are obtained in Fig. 6. It is observed from Fig. 6 that the hourly productivity of both solar distillers had the same behavior of temperature distribution shown in Fig. 5. The productivity of the distillers is lower at times of lower temperatures, and vice versa. For example, the productivity gradually increases from zero as the experiments start at nine o'clock until it reaches its maximum value at 12 o'clock, where the temperature of water and PWPCM recorded their maximum value also at the same time. Besides, it can be seen from Fig. 6 that either the hourly or accumulated productivities were greater than that of the CSS. It was expected that the distillate of MSS with hot feed water, condenser, and PWPCM would be lower than that of the CSS through the charging time, but it was not. This is due to the already high temperature of basin water because of the hot feed water. Therefore, the charging the PWPCM did not affect the water temperature, so the productivity of MSS with hot feed water, condenser, and PWPCM was higher than that of the CSS through the charging time. While, with inverting the slope of solar radiation and temperatures afternoon, the discharging process begins and the PWPCM starts to give thermal energy to the basin water. This boosts to raise the water temperature of MSS with hot feed water, condenser, and PWPCM compared to that of the CSS as shown in Fig. 5. As a result, the evaporation of MSS with hot feed water, condenser, and PWPCM was greater than that of the CSS. Hence, the productivity of MSS with hot feed water, condenser, and PWPCM was more than that of the CSS through the discharging time. The maximum hourly productivity of CSS and MSS with hot feed water, condenser, and PWPCM was 460 and 915 mL/m^2.h at 12:00, respectively. Also, the yield of CSS and MSS reached 85 and 400 mL/m^2.h, respectively at 18:00. In addition, the total yield of MSS with hot feed water, condenser, and PWPCM was more than that of the CSS as illustrated from Fig. 6. The total yield of CSS and MSS with hot feed water, condenser, and PWPCM was 2575 and 6150 mL/m^2.day, respectively. As a result, the MSS with hot feed water, condenser, and PWPCM improved the distillate by around 138.83% over that of the CSS. Also, using the PWPCM only enhanced the productivity by around 33.03% (138.83% for MSS with hot feed water, condenser, and PWPCM – 105.8% for MSS with hot feed water and condenser).

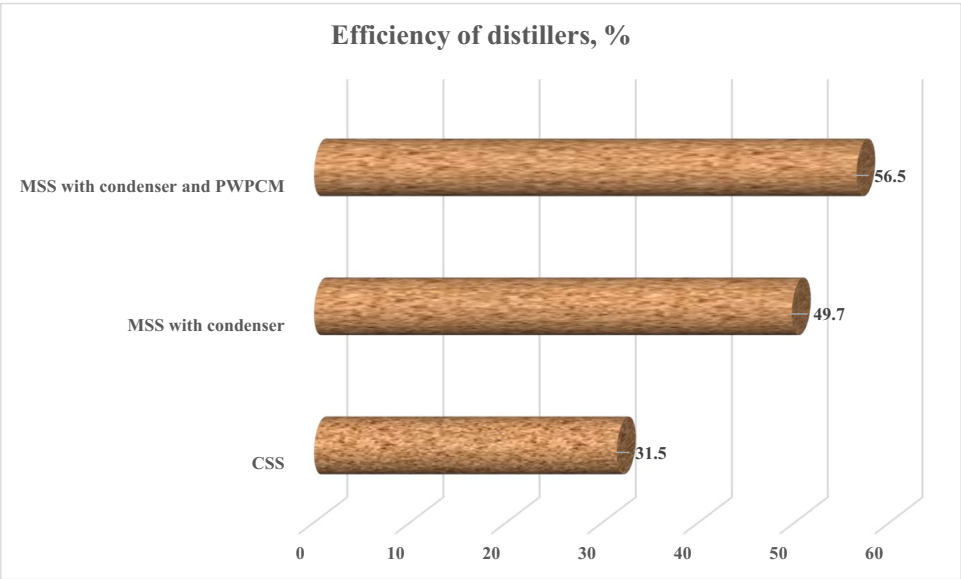

Fig. 7 The efficiencies of solar stills under investigated considerations

Thermal efficiency of distillers under the investigated cases

As well known, the thermal efficiency is the most important parameter for the solar desalination systems to be able to evaluate their performances. The thermal efficiency (η_d) of solar still is calculated by (Abdullah et al. 2019; Kabeel et al. 2017);

$$\eta_d(\%) = \frac{\sum \dot{m}(\text{hourly yield } (kg/m^2.h)) \times h_{fg}(\text{latent heat}(J/kg))}{3600 \times \sum A(\text{projected area } (m^2)) \times I(\text{radiation } (W/m^2))} \times 100 \quad (6)$$

the hot feed water and external condenser with the MSS, the thermal efficiency was reported as 49.7% (Fig. 7). Also, the MSS with hot water, condenser and PWPCM had a thermal efficiency of 56.5% as obtained from Fig. 7.

Economic study for the distilled water

The fixed costs (F) for the modified solar still and conventional solar still are 210 and 110 $, respectively. The fixed cost included the cost of the components, fabrication, and production of the system. In addition, the average daily distillate yields for both CSS and MSS were taken as 2575 and 6150 mL/m^2.day, respectively. The lifetime of the proposed system was assumed to be 5 years with operating days of 340 days in a year. Therefore, the total lifetime cost equals

$$\text{Total cost (C)} = \text{Fixed cost (F)} + \text{Variable cost (V)} \quad (7)$$

Also, the variable, operating, and maintenance costs equal;

$$\text{Vasriable cost(V)} = 0.3 \times \text{Fixed cost (F)} \times \text{System lifetime} \quad (8)$$

The efficiencies of solar stills under the investigated considerations are illustrated in Fig. 7. It can be observed from Fig. 7 that the introduced modifications improved the thermal efficiency of distiller compared to that of the CSS. Besides, the thermal efficiency of solar stills had the trend of increase in productivity curve. For instance, the CSS had an average thermal efficiency of 31.5% through all days of investigations. For the efficiency of MSS, it strongly depends on the operating conditions of experiment. For example, when using

So, the total cost (C) of CSS = 110 + (110 × 0.3 × 5) = 275 $, and the total cost (C) of MSS = 210 + (210 × 0.3 × 5) = 525 $.

Also, the yield of CSS during its lifetime is 340 × 2575 × 5 = 4377.5L. Also, the yield of MSS during its lifetime is 340 × 6150 × 5 = 10455L.

As a result, the potable water cost of 1 L from CSS = 275/4377.5 = 0.063 $. Moreover, the potable water cost of 1 L from MSS = 525/10455 = 0.050 $.

Therefore, the water costs of 1 L from the CSS and MSS are 0.063 $ and 0.050 $, respectively.

Comparison between the results of current and previous studies

A comparison between the results of current and previous studies is obtained in Table 6. This comparison is conducted to obtain the feasibility of the introduced system among the relevant systems. Based on the data of Table 6, the present desalination system is reliable and feasible for operation as compared to other systems.

Table 6 Comparison between the results of current and previous studies

Reference	System with modifications	Increase in productivity	Productivity	Cost of freshwater
(Tiwari et al. n.d.)	Solar still integrated with evacuated tube collector	-	4.2 L/m^2.day	0.022 $/L
(Essa et al. 2021)	Tubular solar still with drum	175%	6.6 L/m^2.day	0.024 $/L
(Abdullah et al. 2021)	Drum still with mirrors and wick	296%	7.25 L/m^2.day	0.041 $/L
(Alawee et al. 2021)	Pyramid still with rotational cylinders and heaters	214%	9.1 L/m^2.day	-
(Abdullah et al. 2019)	Drum still with condensing unit	350%	9.22 L/m^2.day	0.039 $/L
(Elashmawy 2017)	Tubular still + parabolic concentrator + tracking	676%	4.71 L/m^2.day	0.024 $/L
(Essa et al. 2022)	Tubular still with drum, nanoparticles, concentrator, and PCM	218%	6.6 L/m^2.day	0.024 $/L
(Abdullah et al. 2020)	Trays still with mirrors	95%	4.8 L/m^2.day	0.021 $/L
Present study	Incorporated PTSC with MSS	138.83%	6.15 L/m^2.day	0.050 $

Conclusions

Through this work, the performance of a hybrid solar desalination system was investigated. The system consisted of parabolic trough solar collector (PTSC), automatic solar tracking system (ASTS), separation room (SR), modified solar still (MSS), two condensation units (CU), feed water tank (FWT), and supplementary and measuring tools. The impacts of using various water flow rates on the PTSC effectiveness were tested. Also, the influences of integrating condenser to the MSS with and without PWPCM were studied. The experimental results revealed that the best flow rate for PTSC was obtained as 10 L/h (100 L/day), where the EP effectivity was 61%. Under this condition, the obtained freshwater was around 61 L/day from a total saline water of 100 L/day. In addition, integrating a condenser to the MSS improved its productivity, where the total yields of CSS and MSS were 2500 and 5145 mL/m^2.day, respectively. Therefore, the distillate of MSS was improved by 105.8% over that of the CSS due to using the hot feed water and external condenser. Moreover, using PWPCM enhanced the MSS yield. The total yield of CSS and MSS with hot feed water, condenser, and PWPCM was 2575 and 6150 mL/m^2.day, respectively. So, the MSS with hot feed water, condenser, and PWPCM improved the distillate by around 138.83% over that of the CSS. Finally, the CSS had an average efficiency of 31.5%. Also, when using the hot feed water and external condenser with the MSS, the thermal efficiency was reported as 49.7%. Also, the MSS with hot water, condenser and PWPCM had a thermal efficiency of 56.5%. Finally, the water costs of 1 L from the CSS and MSS are 0.063 $ and 0.050 $, respectively.

Acknowledgements The author would like to gratefully acknowledge the financial support by Taif University Researchers Supporting Project number (TURSP-2020/205), Taif University, Taif, Saudi Arabia.

Author contribution Mishal Alsehli—Conceptualization, Methodology, and Writing.

Funding This work was supported by Taif University Researchers Supporting, Project number (TURSP-2020/205).

Data availability Not applicable.

Declarations

Ethical approval Not applicable.

Consent to participate Not applicable.

Consent for publication Not applicable.

Competing interests The author declares no competing interests.

References

Abdelgaied M, Zakaria Y, Kabeel AE, Essa FA (2021) Improving the tubular solar still performance using square and circular hollow fins with phase change materials. Journal of Energy Storage 38:102564

Abdullah AS, Essa FA, Omara ZM, Rashid Y, Hadj-Taieb L, Abdelaziz GB, Kabeel AE (2019) Rotating-drum solar still with enhanced evaporation and condensation techniques: comprehensive study. Energy Conversion and Management 199:112024

Abdullah AS, Younes MM, Omara ZM, Essa FA (2020) New design of trays solar still with enhanced evaporation methods – comprehensive study. Sol Energy 203:164–174

Abdullah AS, Omara ZM, Alarjani A, Essa FA (2021) Experimental investigation of a new design of drum solar still with reflectors under different conditions. Case Studies in Thermal Engineering 24:100850

Abdullah AS, Alawee WH, Mohammed SA, Alqsair UF, Dhahad HA, Essa FA, Omara ZM (2022) Performance improvement of tubular solar still via tilting glass cylinder, nano-coating, and nano-PCM: experimental approach. Environ Sci Pollut Res

Aboelmaaref MM, Zayed ME, Zhao J, Li W, Askalany AA, Ahmed MS, Ali ES (2020) Hybrid solar desalination systems driven by parabolic trough and parabolic dish CSP technologies: Technology categorization, thermodynamic performance and economical assessment. Energy Convers Manage 220:113103

Alawee WH, Mohammed SA, Dhahad HA, Abdullah A, Omara Z, Essa F (2021) Improving the performance of pyramid solar still using rotating four cylinders and three electric heaters. Process Saf Environ Prot 148:950–958

Amarloo A, Shafii MB (2019) Enhanced solar still condensation by using a radiative cooling system and phase change material. Desalination 467:43–50

Elashmawy M (2017) An experimental investigation of a parabolic concentrator solar tracking system integrated with a tubular solar still. Desalination 411:1–8

Emran NY, Ahsan A, Al-Qadami EH, El-Sergany M, Shafiquzzaman M, Imteaz M, Ng A, Tariq M, Idrus S, Mustaffa Z (2022) Efficiency of a triangular solar still integrated with external PVC pipe solar heater and internal separated condenser. Sustainable Energy Technol Assess 52:102258

Essa FA (2022) Thermal desalination systems: from traditionality to modernity and development. Distillation Processes - From Conventional to Reactive Distillation Modeling, Simulation and Optimization. IntechOpen, London, p 23

Essa FA, Abdullah AS, Omara ZM (2021) Improving the performance of tubular solar still using rotating drum – experimental and theoretical investigation. Process Saf Environ Prot 148:579–589

Essa FA, Abdullah AS, Alawee WH, Alarjani A, Alqsair UF, Shanmugan S, Omara ZM, Younes MM (2022) Experimental enhancement of tubular solar still performance using rotating cylinder, nanoparticles' coating, parabolic solar concentrator, and phase change material. Case Studies in Thermal Engineering 29:101705

Faghiri S, Mohammadi O, Hosseininaveh H, Shafii MB (2021) The impingement of liquid boiling droplet onto a molten phase change material as a direct-contact solidification method. Thermal Science and Engineering Progress 23:100888

Faghiri S, Aria HP, Shafii MB (2022) Multi-objective optimization of acetone droplet impingement on phase change material in direct-contact discharge method. Journal of Energy Storage 46:103862

Hassan H, Abo-Elfadl S (2017) Effect of the condenser type and the medium of the saline water on the performance of the solar still in hot climate conditions. Desalination 417:60–68

Holman J (2012) Experimental methods for engineers, 8th edn. McGraw-Hill Companies, New York

Hosseininaveh H, Mohammadi O, Faghiri S, Shafii MB (2021) A comprehensive study on the complete charging-discharging cycle of a phase change material using intermediate boiling fluid to control energy flow. Journal of Energy Storage 35:102235

Kabeel AE, Omara ZM, Essa FA (2017) Numerical investigation of modified solar still using nanofluids and external condenser. J Taiwan Inst Chem Eng 75:77–86

Madhlopa A, Johnstone C (2009) Numerical study of a passive solar still with separate condenser. Renew Energy 34:1668–1677

Makkeh SA, Ahmadi A, Esmaeilion F, Ehyaei M (2020) Energy, exergy and exergoeconomic optimization of a cogeneration system integrated with parabolic trough collector-wind turbine with desalination. J Cleaner Prod 273:123122

Mosleh HJ, Mamouri SJ, Shafii M, Sima AH (2015) A new desalination system using a combination of heat pipe, evacuated tube and parabolic trough collector. Energy Convers Manage 99:141–150

Narayanan SR, Vijay S (2020) Desalination of water using parabolic trough collector. Materials Today: Proceedings 21:375–379

Ranjan K, Kaushik S, Panwar N (2016) Energy and exergy analysis of passive solar distillation systems. International Journal of Low-Carbon Technologies 11:211–221

Shanmugan S, Essa FA, Gorjian S, Kabeel AE, Sathyamurthy R, Muthu Manokar A (2020) Experimental study on single slope single basin solar still using TiO2 nano layer for natural clean water invention. Journal of Energy Storage 30:101522

Srithar K (2010) Performance analysis of vapour adsorptionsolar still integrated with mini-solar pond for effluent treatment. International Journal of Chemical Engineering and Applications 1:336

Tiwari A, Agrawal A, Kumar A. (n.d.) An experimental investigation of a desalination system based on an evacuated tube collector coupled with a heat exchanger. Heat Transfer

Tiwari GN, Sahota L (2017) Advanced solar-distillation systems: basic principles, thermal modeling, and its application. Springer

Ziyaei M, Jalili M, Chitsaz A, Nazari MA (2021) Dynamic simulation and life cycle cost analysis of a MSF desalination system driven by solar parabolic trough collectors using TRNSYS software: a comparative study in different world regions. Energy Convers Manage 243:114412